Pellet fuelling physics studies on MAST

L. Garzotti[1], G. Cunningham[1], J. Figueiredo[2], A. Kirk[1], F. Köchl[3], G. Motojima[4], C. M. Roach[1], M. Valovič[1], D. Dickinson[1,5], C. Gurl[1], G. P. Maddison[1], G. Naylor[1], A. Patel[1], B. Pégourié[6], M. Romanelli[1], R. Scannell[1], G. Szepesi[1,7], A. J. Thornton[1] and the MAST Team

[1]*CCFE, Culham Science Centre, Abingdon, Oxon, OX14 3DB, UK*
[2]*IST, Av. Rovisco Pais, Lisboa, 1049-001, Portugal*
[3]*Österreichische Akademie der Wissenschaften, Austria*
[4]*National Institute for Fusion Science, Toki, Gifu, 509-5292, Japan*
[5]*York Plasma Institute, Department of Physics, University of York, Heslington, York, YO10 5DD, UK*
[6]*Commissariat à l'Énergie Atomique, CE Cadarache, St-Paul-lez-Durance, F-13108, France*
[7]*Centre for Fusion, Space and Astrophysics, University of Warwick, Coventry, CV4 7AL, UK*

Introduction

Pellet injection is foreseen to be the main plasma fuelling technique in large experimental tokamaks like ITER or prototype reactors like DEMO. In order to design an efficient pellet injection system it is important to understand and model the pellet ablation (the process whereby the pellet evaporates in the plasma), the pellet deposition (the fast transport processes redistributing the pellet material inside the plasma) and the post-pellet transport (the way the density and temperature profiles perturbed by the pellet injection relax towards the pre-pellet values).

All these three aspects of pellet-plasma interaction physics have been addressed on MAST. Deuterium pellets of size of the order of 20-30% of the total plasma mass have been injected vertically from the high-field side into a variety of MAST H-mode plasmas with a pneumatic pellet injector at speeds variable between 250 and 400 m/s and pellet penetration has been tuned to be around 0.7-0.8 r/a. In this way we were able to keep the depth of the deposition profile close to the one expected in ITER. Extensive data have been collected with a series of diagnostics, among which the event-triggered Thomson scattering system allows high spatial and temporal resolution measurements of the evolution of the electron density and temperature profile during a pellet injection cycle (pellet ablation and subsequent profile relaxation).

In this paper we review and discuss the results obtained on MAST including data from the latest MAST experimental campaign.

Pellet deposition and ∇B-drift

The Thomson scattering data have been analysed to assess the importance of fast transport of pellet material during the deposition process – a mechanism which is critical in future devices like ITER and appears to depend on machine size; it is stronger on MAST and DIII-D than on JET and Tore-Supra. Figure 1 shows the pre- and post-pellet profiles for MAST shot 24743 compared with the simulations obtained with the pellet ablation/deposition code HPI2 described in [1]. The HPI2 runs were performed taking into account the pre-cooling effect that the drifting cloud has on the target plasma. It can be seen that the pellet deposition cannot be explained by the ablation process alone and, in this particular case, it is compatible with the average drift of ~15 cm predicted by the code. This confirms results reported previously, where drift lengths of the order of 10 cm had been observed in agreement with the HPI2 calculations [2]. However, it should be noted that the general agreement between MAST data and HPI2 predictions is only a partial validation of the code, because the results obtained with HPI2 depend critically on the dynamics of the cloud surrounding the pellet and extending along the magnetic field lines. In particular, the acceleration of the pellet material towards the

low field side and along the magnetic field gradient depends on the evolution of the pressure inside the cloud, for which HPI2 has only a simplified zero-dimensional description.

Plasmoid characterization

To constrain and further validate the simulations of the cloud evolution and motion across the plasma, images of the pellet cloud in five spectral channels (Ba-α, wide Ba-β, narrow Ba-β, Ba-γ and continuum) have been recorded and the cloud main parameters, such as density, temperature and size, have been determined. These measurements were performed by means of a fiberscope developed on LHD and installed on MAST for a few experimental sessions. The fiberscope looks at the pellet from an equatorial port as it travels from the top towards the equatorial plane of the machine. The integration time of the fiberscope was 2 μs and the time interval between measurements was 20 μs, allowing a total of about ten measurements during the pellet lifetime. The spatial resolution was 2.6 mm, which allowed to resolve the structure of the cloud close to the pellet. In the region ~3 cm around the pellet, the density of the cloud is in the range 1-4×10^{23} m^{-3} and the temperature in the range 2-4 eV. To compare the measured values with the prediction of HPI2, one should note that spectroscopic measurements are possible only before the plasmoid becomes completely ionised. During this phase HPI2 predicts plasmoid densities in the range 0.5-5×10^{23} m^{-3} and temperatures in the range 1-1.5 eV in reasonable agreement with the experiment. Finally, from the measurements performed on MAST it appears that the size of the plasmoid in the direction perpendicular to the magnetic field is ~5 cm, which tends to be bigger than observed in other tokamaks.

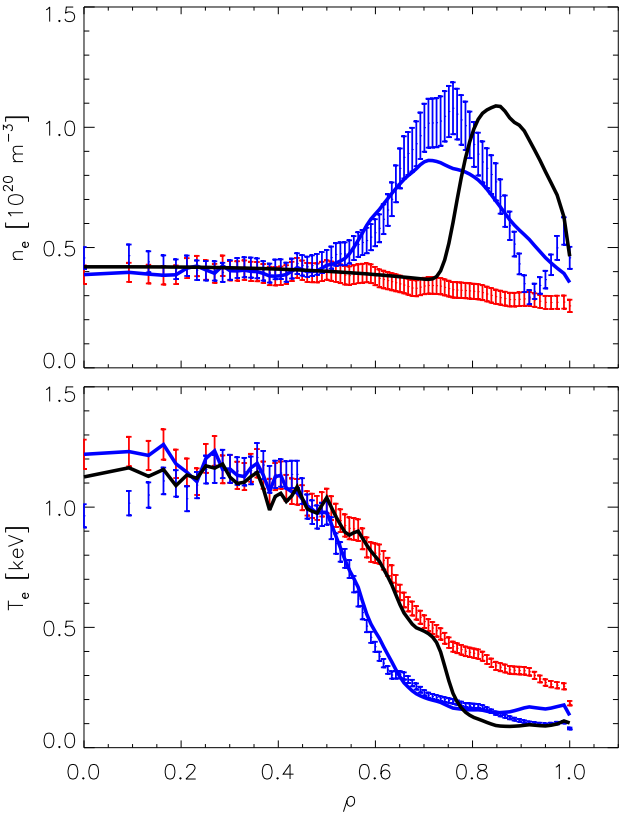

Figure 1: pre- and post-pellet density (top) and temperature (bottom) profiles mapped on the normalized minor radius for MAST shot 24743. Experimental pre-pellet (red bars) and post-pellet (blue bars) profiles. Post-pellet profiles calculated by HPI2 including VB-drift and precooling (blue line) and ablation only (black line).

Post pellet profile relaxation

To study the post-pellet profile relaxation we concentrated on two main phenomena: the effect of the ELMs, which intermittently erode the density profile, and the microstability properties of the post-pellet profile, which determine the inter-ELM transport.

The effect of ELMs on the relaxation of the density profile has been tested experimentally in discharges with and without ELM mitigation by means of resonant magnetic perturbations (RMPs) [3]. Our data show that pellet fuelling and RMP ELM mitigation can be compatible in the sense that the size of post-pellet ELMs responds to ELM mitigation and the post-pellet ELMs are not significantly larger than pre-pellet ELMs. However, it should be noted that, in

our experiments, the relative size of post-pellet ELMs is still quite large and 2-3 ELMs are sufficient to remove the material deposited by single pellet - i. e. a much smaller number of ELMs than expected in ITER. The footprint of an ELM on the post-pellet profile is shown in figure 2, where the pre- and post-ELM density profiles are shown before and after pellet injection for weak and strong ELM mitigation respectively. It can be seen that the ELMs remove particle from the region $\rho > 0.7$-0.8 towards the edge of the plasma. The size of the ELM depends on the strength of the RMP but the width of the region affected by the ELM is not sensitive to it. It is also worth mentioning that, whereas a pre-pellet ELM acts on a flat density profile, a post-pellet ELM affects a hollow density profiles and removes particle even from the region with positive density gradient, suggesting a non-diffusive transport mechanism.

The exceptional space and time resolution of the MAST Thomson scattering system has also allowed an equilibrium reconstruction accurate enough to perform microstability analysis of the post pellet profiles. The analysis was performed with the local gyrokinetic code GS2, which solves the gyrokinetic Vlasov/Maxwell system of equations in toroidal plasmas for an arbitrary number of plasma species in reduced volume flux-tube geometry that is aligned with the equilibrium magnetic field. GS2 includes electromagnetic perturbations and collisions, which are described by means of an energy and pitch angle scattering operator. For the purpose of this study, linear electromagnetic GS2 runs with five species (electrons, D ions, H ions, fast D ions and C ions) were performed for three spatial locations and show a complex interplay between ion temperature gradient (ITG) modes, trapped electron modes (TEMs) and microtearing modes (MTMs), sensitive to the direction of the particle drifts and governed by the large changes in the density and temperature gradients, collisionality and β induced by the pellet. In particular, at the innermost location, corresponding to the part of the pellet deposition profile where the density gradient is positive, all modes are stabilized after pellet injection by the reduction in η_i and η_e (induced by the increased density gradient) and by the favourable magnetic drifts. The picture for the pellet ablation peak (where the density gradient is small or negative) and beyond this radius is more complex. For low $k_y\rho_i$, ITG modes, which dominate before pellet injection, are stabilized, either by increased collisionality, at the pellet ablation peak where $dn/dr \approx 0$, or by reduced η_i, where $dn/dr < 0$. At the

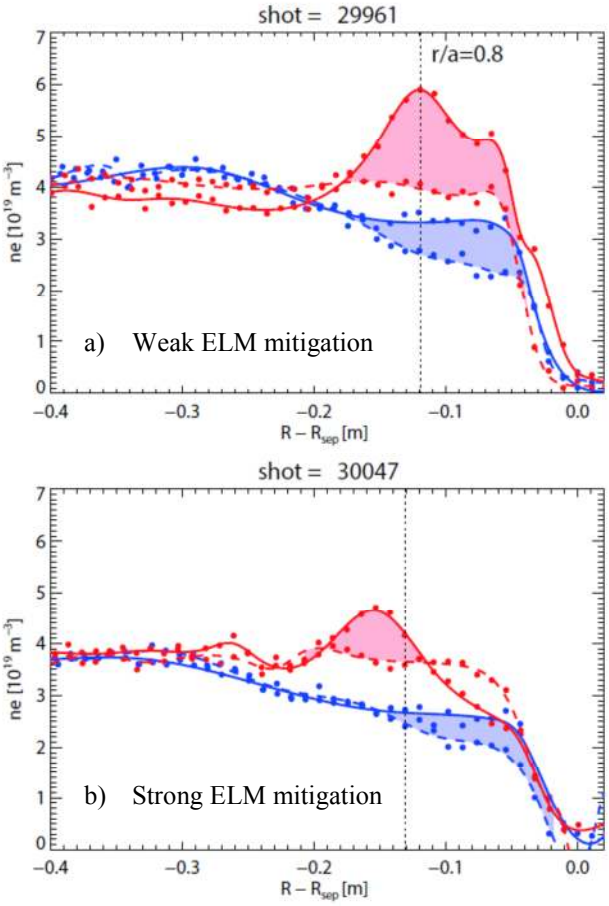

Figure2: density loss due to pre (blue) and post (red) pellet ELMs in presence of ELM mitigation by means of RMPs. a) weak ELM mitigation, b) strong ELM mitigation.

same time MTMs, which are unstable but subdominant before pellet injection, become dominant and can be driven more unstable by the increased β_e. After pellet injection, TEMs are driven unstable by the increased density gradient at the outer surface, where drifts are unfavourable (whereas TEMs were stabilized on the inner surface where the drift opposes the electron diamagnetic flow velocity). Finally, ETG modes remain unstable at the peak of the ablation profile but are stabilized at the outer surface where $dn/dr < 0$ by the reduced η_e. From the fuelling point of view this would imply that, in absence of ELMs, if the density gradients inside the ablation peak are too steep, an asymmetric evolution of the density profile should be expected whereby the anomalous diffusion of the pellet material towards the plasma core would be suppressed by the stabilization of the microturbulence and the pellet particles would diffuse preferentially towards the plasma edge. The results of this study show that it is important to diagnose carefully the evolution of the density and temperature profiles in present day experiments in order to unveil the role of microinstabilities and to assess the performance of physics based transport models. The underlying physics is complex and could lead to different results on different machines (e. g. ASDEX-U or JET) depending on the details of the experiment.

Conclusions

Different aspects of pellet fuelling physics have been studied on MAST. In particular, the physics of pellet ablation and deposition, pellet cloud evolution and post-pellet profile relaxation has been addressed. The results have confirmed the existence of a fast ∇B-drift displacing the pellet material towards the low field side of the tokamak and increasing the deposition depth for pellets injected from the high field side of the plasma. Experimental observations of the pellet deposition depth are in general agreement with the prediction of the HPI2 ablation/deposition code. Moreover, the density and temperature of the pellet cloud predicted by the code are in reasonable agreement with the experimental values derived from spectroscopic measurements. Post pellet relaxation has been studied both during and between ELMs mitigated by RMPs. ELMs remove particle from the region $\rho > 0.7$-0.8 affecting a significant portion of the pellet deposition profile. Between ELMs transport is dominated by microinstabilities and the profile evolution is the result of a complex interplay between different modes. MAST results indicate that inter-ELM transport could be asymmetric and lead to particle diffusion predominately towards the edge of the plasma. However, these results are sensitive to the changes in density and temperature gradients, collisionality and β and could be different on different machines. Nevertheless, they highlight the need for a transport model that captures the physics governing the evolution of the hollow density profiles induced by pellet fuelling.

Acknowledgements

This work was part-funded by the RCUK Energy Programme (grant number EP/I501045) and by the European Union's Horizon 2020 research and innovation programme (grant number 633053). The views and opinions expressed herein do not necessarily reflect those of the European Commission.

References

[1] B. Pégourié *et al* 2007 *Nucl. Fusion* **47** 44
[2] L. Garzotti *et al* 2010 *Nucl. Fusion* **50** 105002
[3] M. Valovič *et al* submitted to *Nucl. Fusion*
[4] L. Garzotti *et al* 2014 *Plasma Phys. Control. Fusion* **56** 035004